CONTROL AND OPTIMIZATION OF THE ELECTROMAGNETIC SUSPENSION OPERATION OF A MAGLEV VEHICLE

José Jaime da Cruz,
Anselmo Bittar,
Eduardo Alves da Costa and
Roberto Moura Sales.
Telecommunications and Control Engineering Department, University of Sao Paulo.
Av. Prof. Luciano Gualberto, trav.3, n. 158, CEP 05508-900, S.P., BRAZIL.
e-mail: jaime@lac.usp.br, anselmo@lac.usp.br, eduardo.costa@poli.usp.br and roberto@lac.usp.br .

Abstract. In this work a control strategy is proposed for levitation of an electromagnetic suspension vehicle prototype. Since the prototype has more actuators than control variables, an optimal distribution of forces among them is performed in order to produce the force and moments required for prototype levitation. The goal is to minimize the maximum force among all the actuators. The reduction of power consumption is the main motivation of the proposed strategy. To stabilize the closed-loop system, a controller with a lead-lag phase characteristic was implemented. The experimental results obtained show that the closed-loop system is stable and exhibits a satisfactory transient response.

Keywords. MAGLEV vehicle, levitation control, optimization, electromagnetic suspension.

1. Introduction

MagLev vehicles constitute a new class of high speed transport systems that has been constantly developed and improved to become a new alternative of fast and secure transport. These vehicles have suspension, propulsion and guidance systems based on magnetic forces (Bohn et al., 1984; Glatzel et al., 1980; Jayawant, 1982; Meins et al., 1988; Moon, 1994 and Sinha, 1987).

In this work, an electromagnetically levitated vehicle prototype as shown in Fig. (1) is considered. Levitation can be accomplished with the action of attraction forces produced by electromagnets (Bittar et al. 1997-1998). In this type of suspension levitation may be attained at any speed since the attraction force is independent of it. On the other hand the levitation phenomenon is unstable and the electromagnetic force is nonlinear giving rise to difficulties to get closed-loop stability.
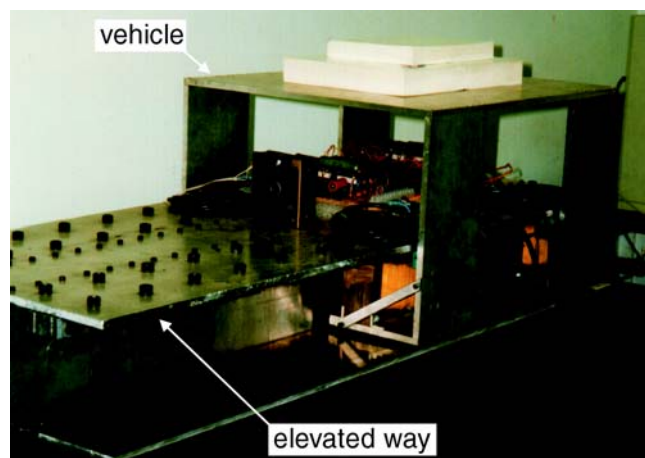

Figure 1: MagLev vehicle prototype photograph.

Four electromagnets are located at the corners of the prototype to produce the attraction forces and four inductive sensors are used to measure the gaps of the electromagnets. The prototype scheme is presented in Fig. (2).
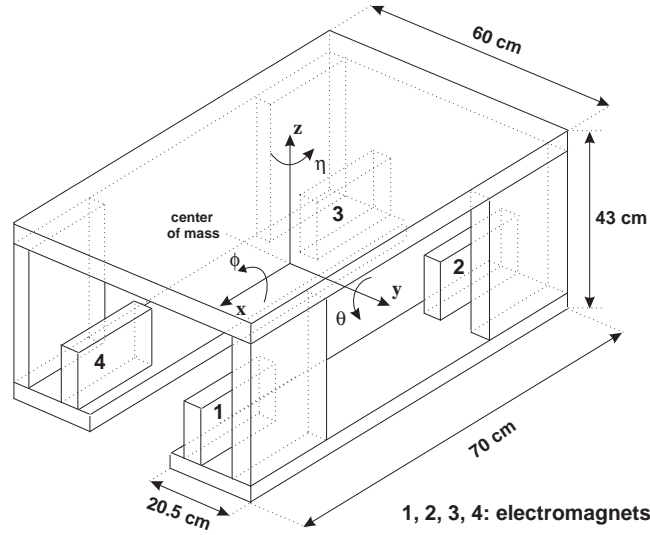

Figure 2: Vehicle scheme.

The prototype will have independent levitation, guidance and propulsion systems but only levitation is considered in this paper. The system is modelled assuming rigid body dynamics. Levitation is achieved by controlling its three degrees of freedom, namely, heave $z(t)$, roll $\phi(t)$ and pitch $\theta(t)$. Since in normal operation these variables are small, the system equations can be linearized around the reference equilibrium point (z_{ref}, $\phi_{\mathrm{ref}} = 0$, $\theta_{\mathrm{ref}} = 0$). Three decoupled SISO systems then result for which the vertical force $F_z(t)$ and the moments $M_x(t)$ and $M_y(t)$ are the control variables.

At least four electromagnets are required for vehicle levitation since the electromagnetic forces are attractive and both positive as well as negative moments $M_x(t)$ and $M_y(t)$ may be necessary to control roll and pitch angles. An optimization problem is defined to evaluate the forces to be produced by the four electromagnets in order to get the three control variables above. The goal is to minimize the maximum force among all the actuators.

Four inductive sensors are used to measure the gaps of the electromagnets. This choice improves the quality of the measurement system since just three of them would be sufficient. Such redundancy also increases system reliability to sensor faults. The controller inputs ($z(t)$, $\phi(t)$ and $\theta(t)$ errors) are evaluated using the measured gaps ($z_j(t)$, $j = 1, \ldots, 4$).

In practice the levitation of electromagnetic suspension vehicles has a large number of actuators. The levitation control based on three SISO systems together with an optimal operation of the actuators may be used to improve system reliability by redistributing the forces in case of actuator faults. It is also expected that the proposed control scheme reduces the energy consumption required for levitation since power loss in each electromagnet is roughly proportional to its electromagnetic force.

Tab. (1) contains some prototype data.

Table 1. Prototype data.

Length	70 cm	Nominal air gap	0.005 m
Width	60 cm	Levitation power	377 W
Height	43 cm	Supply voltage	55 VDC
Vehicle mass	97.6 kg	Steady state current in each coil	1.71 A

The paper is organized as follows. Section 2 discusses briefly the prototype actuators. Section 3 contains the system model. Section 4 describes the optimal operation of the actuators. In section 5 the measurement processing to estimate the three controller inputs from the four measured gaps is presented. A brief description of the SISO controller for each degree of freedom is made in section 6. Section 7 contains the experimental results. The main conclusions are then summarized in section 8.
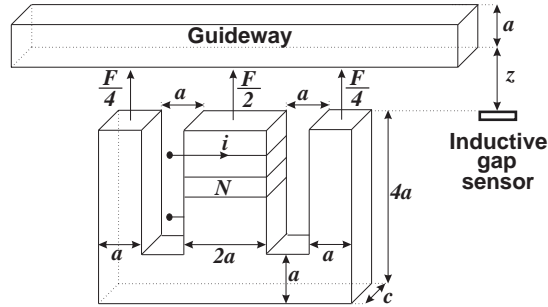
2. Prototype Actuators

Figure 3: Electromagnet.

Each levitation electromagnet has an "E" shape as shown in Fig. (3) and its attraction force is given by

$$F(t) = k_f \left(\frac{i(t)}{z(t)} \right)^2 \tag{1}$$

where $i(t)$ is the current, $z(t)$ is the air gap and k_f is a constant.

For a given air gap $z(t)$ the electromagnetic force is thus proportional to the current squared. Hence the levitation power loss in a given actuator can be minimized by minimizing its electromagnetic force.

The choice of the steady state gap is directly related to the conflicting requirements of energy consumption and performance of the levitation control system. From the point of view of energy consumption, it would be interesting to set the gap as small as possible since the current required for vehicle levitation would be proportionally small. On the other hand the coil inductance would also be high difficulting a fast control action. Furthermore small gaps may give rise to magnetic saturation.
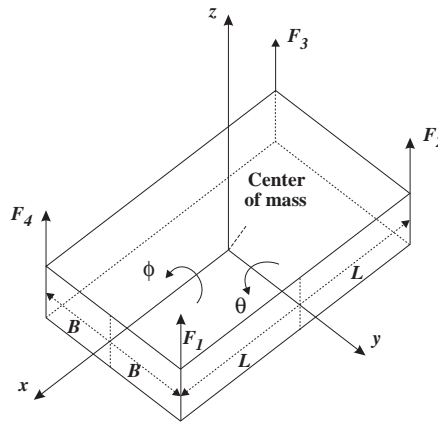
3. System Modelling

Figure 4: Scheme of forces.

Fig. (4) shows a scheme of forces for prototype levitation. A dynamical model for this system can be easily written if we assume rigid body dynamics and the occurrence of small displacements around the equilibrium point represented by a given z_{ref}, $\phi_{\text{ref}} = 0$ and $\theta_{\text{ref}} = 0$:

$$M\ddot{z}(t) = Mg - F_z(t) \tag{2}$$

$$I_{xx}\ddot{\phi}(t) = M_x(t) \tag{3}$$

$$I_{yy}\ddot{\theta}(t) = M_y(t) \tag{4}$$

where $F_z(t)$ is the resultant vertical force, $M_x(t)$ and $M_y(t)$ are the components of the moment along the x and y axes, respectively, I_{xx} and I_{yy} are the corresponding moments of inertia, M is the vehicle mass and g is the local gravity acceleration. In the present case, $M = 97.6$kg, $I_{xx} = 5.9$kgm^2 and $I_{yy} = 7.9$kgm^2.

The dynamical model has thus the form of a decoupled system of linear equations. Heave, roll and pitch dynamics are given respectively by equations (2), (3) and (4).

As shown in the closed-loop system block diagram of Fig. (5), the gap z(t) has to be regulated around a given reference value z_{ref} whereas both roll $\phi(t)$ and pitch $\theta(t)$ angles have to be regulated around zero.
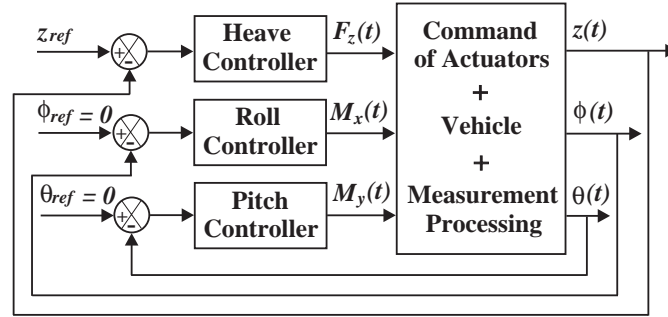

Figure 5: Closed-loop system block diagram.

The system dynamical model has thus three inputs ($F_z(t)$, $M_x(t)$ and $M_y(t)$) and three outputs ($z(t)$, $\phi(t)$ and $\theta(t)$). On the other hand the prototype has four inputs ($i_j(t)$, $j = 1, \ldots, 4$) and four outputs ($z_j(t)$, $j = 1, \ldots, 4$).

To fully compatibilize the variables of the problem, two blocks, namely, command of actuators and measurement processing, are defined and included in the control loop. As indicated in Fig. (6), the inputs to the first block are the control variables generated by heave, roll and pitch controllers; its outputs are the currents to be applied to the electromagnets. The measurement processing block must compute the values of heave as well as of both roll and pitch angles based on the four gap measurements.

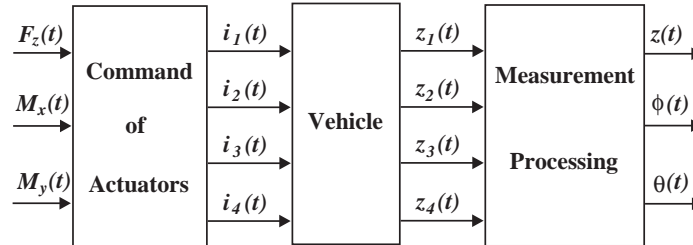A detailed exposition of the contents of these blocks is done in the following sections.

Figure 6: Detail of the system diagram.

4. Optimal Operation of Actuators

The purpose of the command of actuators is, at each time t, to compute the four electromagnetic forces $(F_1(t),\ F_2(t),\ F_3(t),\ F_4(t))$ in order to produce the three control variables $(F_z(t),\ M_x(t),\ M_y(t))$ required by the SISO controllers. The indetermination present in this problem can be removed by defining an optimization problem.

Let $F_u(t)$ be an upper bound on the electromagnets forces:

$$F_u(t) \geq F_1(t),\ F_2(t),\ F_3(t),\ F_4(t) \ . \tag{5}$$

The goal is to minimize $F_u(t)$ subject to the constraints that follow. For sufficiently small roll $\phi(t)$ and pitch $\theta(t)$ angles, the following approximations hold

$$F_z(t) = F_1(t) + F_2(t) + F_3(t) + F_4(t) \ , \tag{6}$$

$$M_x(t) = (F_1(t) + F_2(t) - F_3(t) - F_4(t))B \ , \tag{7}$$

$$M_y(t) = (-F_1(t) + F_2(t) + F_3(t) - F_4(t))L \ . \tag{8}$$

where B and L are the lengths shown in Fig. (4).

Since the electromagnets produce only attraction forces, the following additional constraints must be included

$$F_1(t),\ F_2(t),\ F_3(t),\ F_4(t) \geq 0 \ . \tag{9}$$

The solution of the Linear Programming Problem (LPP) of minimizing $F_u(t)$ subject to the set of constraints of equations (5)-(9) can be obtained analytically. From equations (6)-(8) it follows that

$$
\begin{aligned}
F_1(t) &= a_1(t) - F_4(t) \ , &(10)\\
F_2(t) &= a_2(t) + F_4(t) \ , &(11)\\
F_3(t) &= a_3(t) - F_4(t) \ , &(12)
\end{aligned}
$$

where

$$a_1(t) \triangleq \frac{1}{2}\left(F_z(t) - \frac{M_y(t)}{L}\right) \ , \tag{13}$$

$$a_2(t) \triangleq \frac{1}{2}\left(\frac{M_x(t)}{B} + \frac{M_y(t)}{L}\right) \ , \tag{14}$$

$$a_3(t) \triangleq \frac{1}{2}\left(F_z(t) - \frac{M_x(t)}{B}\right) \ . \tag{15}$$

Using equations (10)-(12) and defining

$$b_1 \triangleq \max\{\, 0\ ,\ -a_2 \,\} \geq 0 \ , \tag{16}$$

$$b_2 \triangleq \min\{\, a_1\ ,\ a_3 \,\} \geq 0 \ , \tag{17}$$

the constraints (9) can be rewritten as

$$
\begin{aligned}
F_4(t) &\geq b_1 \ , &(18)\\
F_4(t) &\leq b_2 \ . &(19)
\end{aligned}
$$

Similarly, defining

$$b_3 \triangleq \max\{\, a_1\ ,\ a_3 \,\} \geq 0 \ , \tag{20}$$

$$b_4 \triangleq \min\{\, 0\ ,\ -a_2 \,\} \leq 0 \ , \tag{21}$$

inequalities (5) can be rewritten as

$$
\begin{aligned}
F_u(t) &\geq -F_4(t) + b_3 \ , &(22)\\
F_u(t) &\geq F_4(t) - b_4 \ . &(23)
\end{aligned}
$$

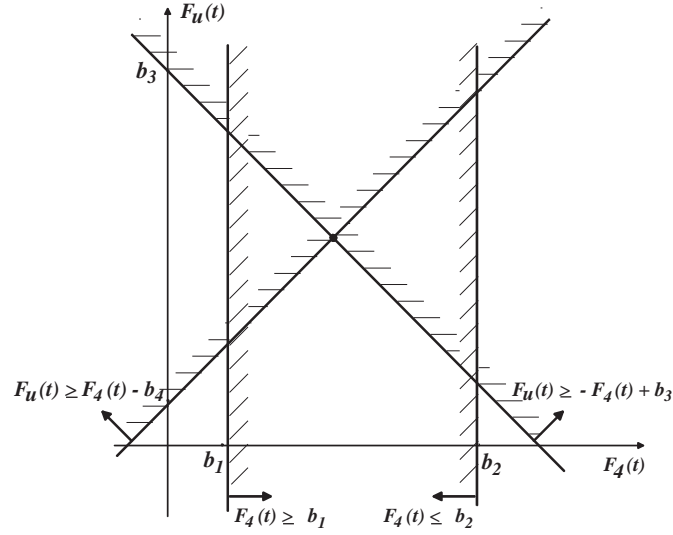Fig. (7) illustrates the constraints (18), (19), (22) and (23) on $F_u(t)$ and $F_4(t)$.

Figure 7: Constraints on $F_u(t)$ and $F_4(t)$.

Since the goal is to minimize $F_u(t)$, a straightforward analysis of this figure leads to the optimal solution $F_4^*(t)$:

$$\frac{b_3 + b_4}{2} < b_1 \Rightarrow F_4^*(t) = b_1 , \tag{24}$$

$$b_1 \leq \frac{b_3 + b_4}{2} \leq b_2 \Rightarrow F_4^*(t) = \frac{b_3 + b_4}{2} , \tag{25}$$

$$b_2 < \frac{b_3 + b_4}{2} \Rightarrow F_4^*(t) = b_2 . \tag{26}$$

Substituting $F_4^*(t)$ into equations (10)-(12) the problem is solved.
A straightforward analysis shows that $b_1 \leq b_2$. The optimization problem has thus always a solution.

5. Measurement Processing

The purpose of the measurement processing described in the following is to evaluate the gap $z(t)$ and the angles $\phi(t)$ and $\theta(t)$, using the measurements of the four gaps taken by the sensors.
The heave displacement $z(t)$ is given by the mean value of the four measured gaps:

$$z(t) = \frac{1}{4}(z_1(t) + z_2(t) + z_3(t) + z_4(t)). \tag{27}$$

Fig. (8) shows a sketch of the section of the vehicle contained in the $y - z$ plane (see Fig. (4)).
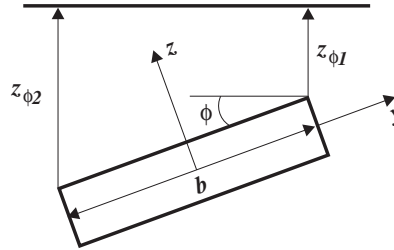

Figure 8: Section of the vehicle in the $y - z$ plane with roll angle shown.

Assuming small deviations of the gaps from the reference value and defining

$$z_{\phi 1}(t) = \frac{z_1(t) + z_2(t)}{2}, \tag{28}$$

$$z_{\phi 2}(t) = \frac{z_3(t) + z_4(t)}{2}, \tag{29}$$

the angle $\phi(t)$ can be approximated by

$$\phi(t) \cong \frac{z_{\phi 2}(t) - z_{\phi 1}(t)}{b}, \tag{30}$$

where b is the distance between the sensors measured along axis y.

In the same way, after defining

$$z_{\theta 1}(t) = \frac{z_2(t) + z_3(t)}{2}, \tag{31}$$

$$z_{\theta 2}(t) = \frac{z_1(t) + z_4(t)}{2}, \tag{32}$$

an approximation for $\theta(t)$ can be written as

$$\theta(t) \cong \frac{z_{\theta 2}(t) - z_{\theta 1}(t)}{l}, \tag{33}$$

where l is the distance between the sensors measured along axis x.

Thus, the gap z(t) and both angles $\phi(t)$ and $\theta(t)$ can be estimated using equations (27), (30) and (33).

6. Controllers

Heave, pitch and roll controllers have been obtained using the H_2/H_∞ theory (Doyle et al. 1989). Their transfer functions are given by

$$G_c(s) = \frac{K_c(s + 0.8)(s + 60.0)(s + 62.6)(s + 100.0)}{s(s + 57.5)(s + 71.5)(s + 301.7 \pm 299.2j)}, \tag{34}$$

where the gain K_c has been tuned for each controller. The controllers have been discretized using the well-known Tustin approximation and implemented in a microcomputer with a sample rate of 3.5 kHz.

It is worth to mention some important features of $G_c(s)$:

• it has a lead-lag phase characteristic;

• occurrence of phase lead in low frequencies which is essential to produce closed-loop stability since the open-loop models have two poles at the origin;

• presence of high-frequency poles to reject sensor noise;

• presence of an integrator to obtain null steady-state error for step inputs at the reference (as in the case of levitation starting) and step disturbances at the plant input (as in the case of load disturbances).

System stabilization for gaps significantly different from the nominal one is difficult: large gaps require excessive electrical power whereas small gaps give rise to high electromagnet inductances difficulting fast control actions.

7. Experimental Results

The closed-loop response for a reference gap of 5 mm has been considered. A step disturbance has been applied to the plant by suddenly laying a mass of 3kg on the vehicle.

Fig. (9) shows the heave, roll and pitch errors. It can be seen that the closed-loop system is stable as expected. The disturbance has been completely rejected in steady-state.

Fig. (10) shows the four gaps as functions of time. The presence of coupling can be clearly observed. Furthermore, all gaps oscillate in phase indicating that the heave resonant frequency of the vehicle is predominant over both roll and pitch ones being less damped than them.

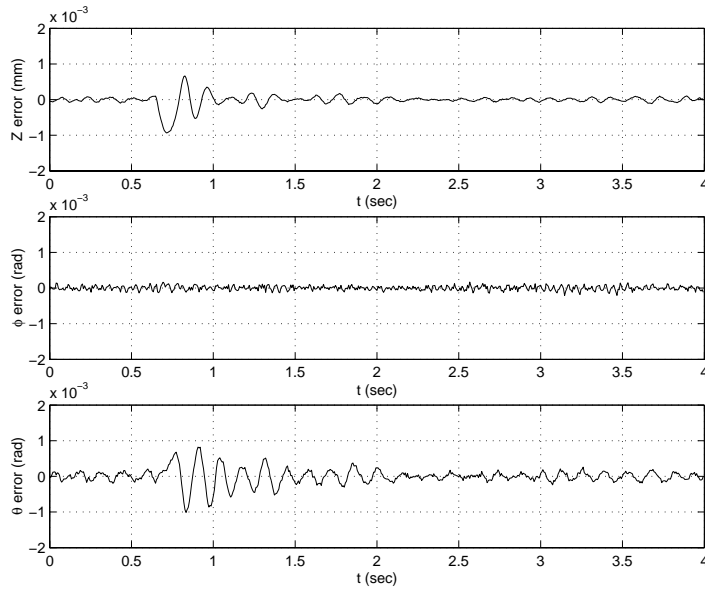Both figures show that the transient response exhibits a settling time of about 0.5 sec.

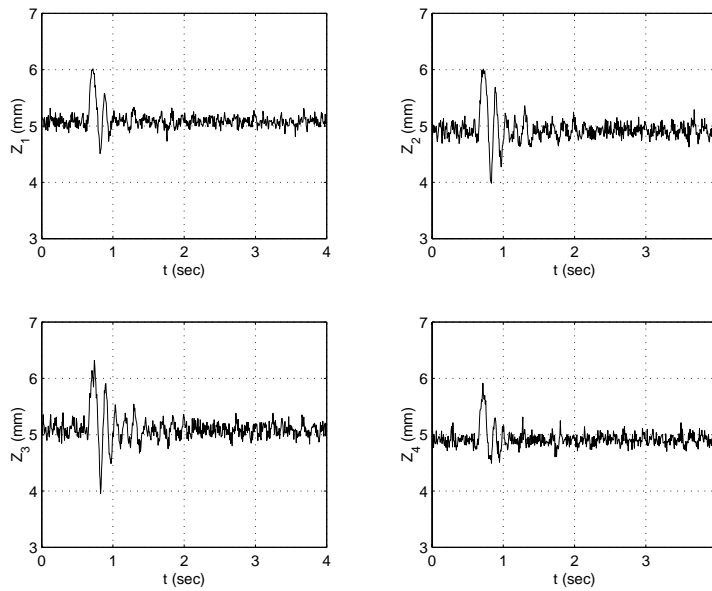Figure 9: z, ϕ and θ error signals as functions of time.

Figure 10: Gaps z_1 to z_4 shown as functions of time.

8. Conclusions

A control approach to the levitation of an electromagnetic suspension vehicle prototype based on the optimal operation of the actuators has been proposed in this paper. The main motivation has been to reduce energy consumption. The control scheme can also be employed to improve system reliability in case of actuators faults.

Experimental results have been shown to illustrate the application of the control approach to a vehicle prototype.

The same approach could be employed in different systems whenever the number of actuators is greater than the the number of control variables. A typical application is the dynamic positioning of offshore platforms using thrusters.

9. Acknowledgements

10. References

Bittar, A. and Sales, R. M., 1997, "H_2 and H_∞ control applied to an electromagnetically levitated vehicle", IEEE International Conference on Control Applications, October 5-7, Connecticut, USA.

Bittar, A. and Sales, R. M., 1997, "Control results for an electromagnetically levitated vehicle prototype", European Control Conference, ECC, July, Belgium.

Bittar, A., Cruz, J. J. and Sales, R. M., 1998, "A New Approach to the Levitation Control of an Electromagnetic Suspension Vehicle", IEEE International Conference on Control Applications, CCA, Italy.

Bittar, A. and Sales, R. M., 1998, "H_2 and H_∞ control for MagLev Vehicles", IEEE Control Systems Magazine, Vol. 18, No. 4, pp.18-25.

Bohn, G. and Steinmetz, G., 1984, "The electromagnetic levitation and guidance technology of the TRANS-RAPID test facility emsland", IEEE Transactions on Magnetics, Vol. MAG-20, N°. 5, pp. 1666-1671.

Doyle, J. C., Glover, K., Khargonekar, P. P. and Francis, B. A., 1989, State-Space Solutions to Standard H_2 and H_∞ Control Problems, "IEEE Transactions on Automatic Control", Vol. AC-34, pp. 831-847.

Glatzel, K., Khurdok G. and Rogg, D., 1980, "The development of the magnetically suspended transportation system in the federal republic of germany", IEEE Transactions on Vehicular Technology, Vol. VT-29, N°. 1, pp. 3-16.

Jayawant, B. V., 1982, "Electromagnetic suspension and levitation", Proceedings of the IEE, Vol. 129, Pt. A, N°. 8, pp. 549-581.

Meins, J., Miller, L. and Mayer, W. J., 1988, "The high speed MAGLEV transportation system TRANSRAPID", IEEE Transactions on Magnetics, Vol. MAG-24, N°. 2, pp. 808-811.

Moon, F. C., 1994, "Superconducting Levitation: Applications to Bearings and Magnetic Transportation", John Wiley and Sons.

Sinha, P. K., 1987, "Electromagnetic suspension: dynamics and control", Peter Peregrinus Ltd, London.